Journal of Molecular and Engineering Materials

DOI: 10.1142/S2251237319500060

Investigation of Structural, Dielectric and Electrical Properties of Barium Titanate Ceramics Co-Doped with Bismuth and Yttrium

Suravi Islam*,§, Syed Abdus Satter†, Nazia Khatun*, Mohammad Sajjad Hossain*, Syed Farid Uddin Farhad*, Parimal Bala†, Samia Tabassum‡ and Ayesha Siddika‡

*Industrial Physics Division
Bangladesh Council of Scientific and Industrial Research
BCSIR, Dhaka 1205, Bangladesh

†Department of Physics
Jagannath University
Dhaka 1000, Bangladesh

‡Institute of Fuel Research Development (IFRD)
BCSIR, Dhaka 1000, Bangladesh
§suravii@yahoo.com

Received 3 September 2019
Accepted 24 September 2019
Published 26 November 2019

Bismuth and Yttrium co-doped Barium Titanate ($BaTiO_3$) ceramics with the general formula $(Ba_{1-x}Bi_X)$ (Y_xTi_{1-x}) O_3 (where $x = 0.00$, 0.01, 0.03, 0.05) have been synthesized at 1300°C for 3 h by the standard solid-state reaction method. The prepared samples were characterized by X-ray diffraction (XRD), Scanning Electron Microscope (SEM) and Impedance Analyzer. Temperature-dependent dielectric properties of the samples were also measured. The XRD result revealed perovskite structure for un-doped and co-doped $BaTiO_3$ with tetragonal phase. However, with increasing doping concentration, a Pseudo cubic phase occurs also confirmed by the twin peaks (002) and (200) of XRD pattern. From SEM micrograph, submicron size particles were observed for all synthesized $BaTiO_3$ samples and exhibit a narrow size distribution with quiet uniform morphology. The crystalline size for un-doped $BaTiO_3$ found was 24.26 nm, the size decreases (minimum 19.59 nm for $x = 0.03$) for all compositions of co-doped $BaTiO_3$. Dielectric constant values were apparently high and direct current (DC) resistivity follows a decreasing trend at higher doping concentration. The sample doped with $x = 0.01$ shows minimum DC resistivity and maximum dielectric constant among the samples investigated.

Keywords: $BaTiO_3$; dielectric properties; DC resistivity; dielectric constant.

§Corresponding author.

1. Introduction

Barium titanate ($BaTiO_3$, BT) has attracted researchers intensively for its ferroelectric properties since its discovery in 1945.[1] The unique physical properties, emphasized dielectric and piezoelectric properties, environment friendly and nontoxic nature of BT has received significant attention for industrial applications.[2–4] Suitably doped BT dielectric ceramics have applications in semiconductors, capacitors, positive temperature coefficients resistors, ultrasonic transducers and piezoelectric devices.[5–7] BaTiO3 has a typical perovskite structure and four modifications: rhombohedral, orthorhombic, tetragonal and cubic. The most important ferroelectric (tetragonal) phase gets converted to paraelectric (cubic) phase at the Curie temperature (T_c) $\sim 120^\circ$C.[8]

There are several methods used for the synthesis of BT, these are solid-state reaction, mechanochemical synthesis and wet chemical methods like sol–gel, hydrothermal, co-precipitation method.[9] Various types of additives are mixed on A and/or B sites of BT powder[8,9] to obtain better performances and a good control over grain sizes, electrical characteristics of ceramics. Dielectric response in rare earth modified BT using co-doping method has been studied widely.[8–10] Bi and Cu co-doped BT was found with $T_c \sim 140^\circ$C at $x = 0.01$ and confirmed by temperature dependence of the dielectric constants.[10] The co-doping of Y and Mn facilitates sintering with the base-metal electrodes as well as improves the device performance and life time.[11] The effect of Mg and Y addition markedly modify the dielectric constant-temperature properties of the $BaTiO_3$.[12]

Previous studies show a number of different dopants (Bi/Cu, Y/Mn, Sm/Mn, Mg/Y, etc.) were used in $BaTiO_3$ to tailor its structural and dielectric properties. To the best of our knowledge, no work has been reported in case of co-doping effect of Bi and Y in Barium Titanate. Here, Bi and Y ions were selected as donor and acceptor substituting for A site & B site of BT-based ceramics, respectively. The aim of this study is to investigate the effect of co-doping on Curie temperature (T_c) and the dielectric properties varying with doping concentration. Also, structural and morphological studies have been analyzed.

2. Materials and Methods

Analytical grade $BaCO_3$ (99.0%), TiO_2 (99.0%), Bi_2O_3 (99.9%) and Y_2O_3 (99.9%, MERCK, Germany) were used as raw materials for the preparation of Bismuth and Yttrium co-doped Barium Titanate ceramics. The samples were prepared according to the stoichiometric equation $(Ba_{1-x}Bi_X)(Y_xTi_{1-x})O_3$ ($x = 0.00$, 0.01, 0.03, 0.05) by a conventional solid-state reaction method. Oxide metals were mixed together and milled by a high-precision planetary ball mill (Fritch Pulverisette 6, Germany) for 6 h in dry atmosphere to get a homogeneous mixture. The weight ratio of ball to sample was 2:1 contained in a bowl (250 ml) where the milling speed was kept at 150 rpm. The mixtures were presintered at 700°C for 3 h in air and again hand milled for half an hour. The grinded BT powders were mixed with 4 wt.%. PVA (Polyvinyl alcohol) aqueous solution, which acts as a binder and was pressed into disk-like pellets with applying pressure of 2 ± 0.5 MPa for 1 min. Finally, the pellets were sintered in a programmable muffle furnace (Nabertherm, Germany) at 1300°C for 3 h in air.

The synthesized samples were characterized by SEM (Hitachi, S-3400N), XRD (EMMA, GBC Scientific equipment radiation functioned at 40 KV and 40 mA, source Cu–kα ($\lambda = 1.54052^\circ$ A) and Impedance Analyzer (Agilent 4294A, 40 kHz to 120 MHz). A two-probe method was used to measure the resistance and capacitance of the sample to get temperature-dependent dielectric properties.

3. Results and Discussion

3.1. *X-ray diffraction (XRD) analysis*

X-ray diffractogram (XRD) is a useful tool to identify various phases of BT Perovskites as well as other structural properties. Powder XRD patterns for $(Ba_{1-x}Bi_X)(Y_xTi_{1-x})O_3$, ($x = 0.00$, 0.01, 0.03, 0.05) samples sintered at 1300°C for 3 h are shown in Fig. 1. Strong peaks were generated from the undoped and Bi-Y co-doped BT confirmed perovskite structure formation and completion of solid-state reaction. From the XRD patterns, the diffraction peaks found have (001), (101), (111), (002), (200), (210), (112), (211) planes at $2\theta \approx 22^\circ$, 32°, 39°, 45.2°, 45.7° and 52°, respectively. Structural evaluation was observed from the main peaks (101) and the characteristic peaks (002, 200).

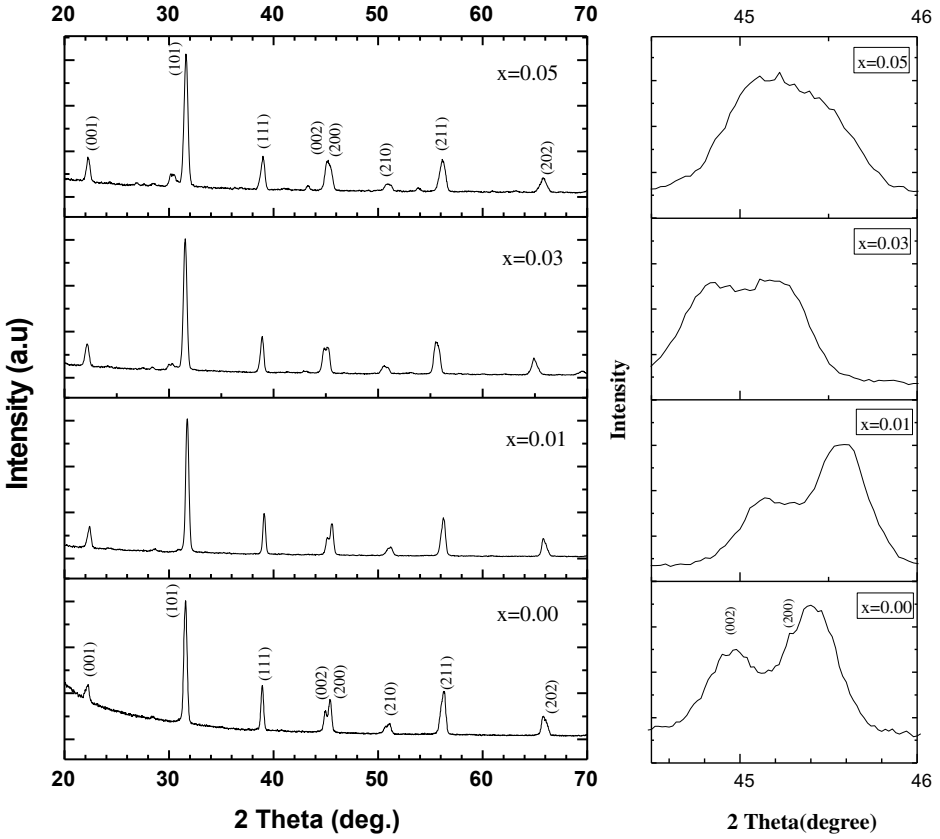

Fig. 1. Powder X- ray diffraction pattern and Gaussian fitting of the peaks in the vicinity of 44.5–46° for $Ba_{1-x}Bi_X$) $(Y_xTi_{1-x})O_3$, (where $x = 0.00, 0.01, 0.03, 0.05$) ceramic samples.

In our experiment, a slight shift of the diffraction peaks toward lesser degree was observed with the increase in Bi and Y doping concentrations. Tetragonal and cubic phase were identified generally by an analysis of the 002 (tetragonal) and 200 (cubic) in the 2θ range of 45–46°. The splitting of 002 and 200 peaks indicates the tetragonal phase, while the single (200) peak confirms the cubic phase. Our experimental results show as doping concentration of Bi and Y in $BaTiO_3$ increased, the intensity of the peak (002) minimized. Hence, shifting of Bragg peak from 45.5 towards 45.0° confirms the phase transition from tetragonal phase to cubic phase after the certain limit of doping concentration that matches with the previous result.[13,14] Though an ideal cubic perovskite structure did not appear by broadening the 200 peak, it may be considered as pseudocubic. Lattice parameter along these twin peaks are calculated and plotted as a separate panel in Fig. 1, where the diminishing effect of tetragonality can be visualized. Loosing tetragonality generally stabilizes the cubic phase, resulting in reduced dielectric constant and similar result was reported for Nb doped BT.[15]

The lattice parameters (a) and (c) were calculated by using Miller indices (hkl) values and

Table 1. Variation of structural parameters: lattice parameter (a) (Å), lattice parameter (c) (Å), tetragonality c/a ratio, Crystal Size and X-ray density for the solid solution of $(Ba_{1-x}Bi_X)$ $(Y_xTi_{1-x})O_3$ samples.

Content of x in $(Ba_{1-x}Bi_X)$ $(Y_xTi_{1-x})O_3$	Lattice parameter (a) (Å)	Lattice parameter (b) (Å)	Lattice parameter (c) (Å)	Tetragonality (c/a)	Crystal size in nm	X-ray density g/m^3
$X = 0.00$	3.992	3.992	4.023	1.00877	24.26	6.03
$X = 0.01$	3.978	3.978	4.014	1.0088	21.87	4.909
$X = 0.03$	4.014	4.014	4.036	1.0055	19.59	5.04
$X = 0.05$	4.010	4.010	4.167	1.039	22.89	4.98

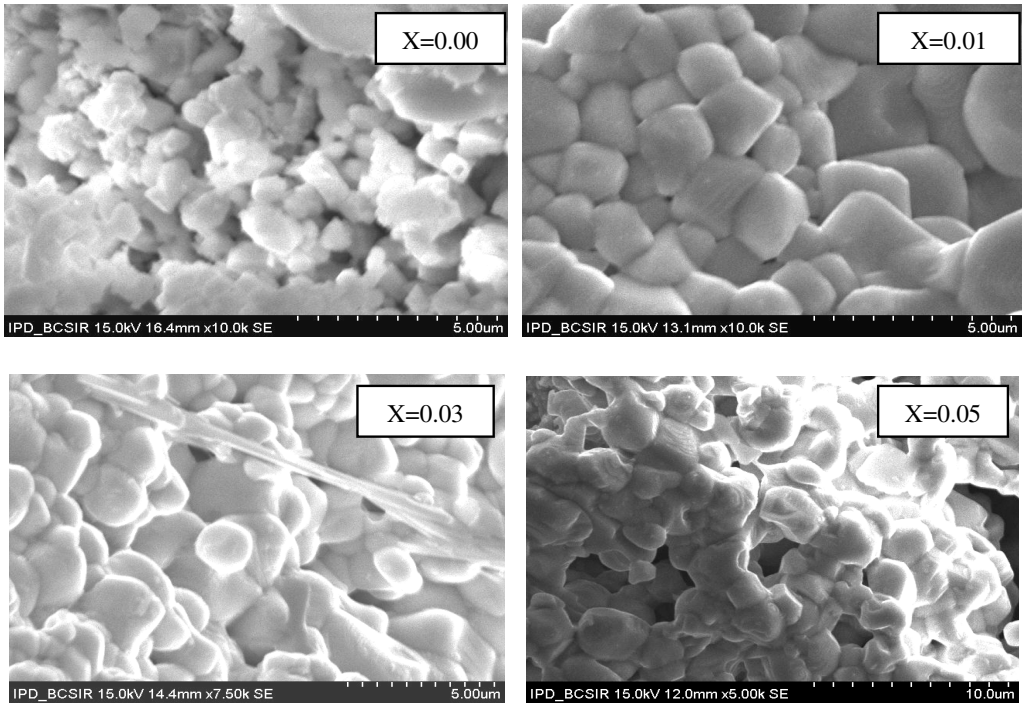

Fig. 2. SEM micrographs of $(Ba_{1-x}Bi_X)$ $(Y_xTi_{1-x})O_3$ samples for different values of x (where $x = 0.00, 0.01, 0.03, 0.05$).

interplanar spacing with the relation $1/d^2 = h^2 + k^2/a^2 + l^2/c^2$; where d is interplanar spacing.[16] The measured lattice parameters a, c and c/a ratio, crystal sizes and X-ray density of the prepared samples are depicted in Table 1.

3.2. *Microstructural characteristics*

The SEM micrographs of the synthesized samples are shown in Fig. 2. It reveals the microstructure of $BaTiO_3$ has effect on Bi and Y addition for all doping concentrations. Submicron size particles were observed with less than 2 μm sizes for each case of doping. Apparently, it demonstrates particle size increases gradually with increasing doping concentration. The average grain size measured from the micrographs are represented in Table 2. Both coarse and fine grain particles were observed and it exhibits a narrow size distribution with quiet uniformity.

Maximum homogeneity for sample $x = 0.01$ was found. The average grain size varies significantly due to doping content, it increases up to a certain limit, estimated minimum 0.59 μm at $x = 0.03$ and maximum 1.85 μm for $x = 0.05$. The grain size has strong influence on the microstructure and dielectric properties of the synthesized samples.[4] The observed microstructures exhibit homogenous grain distribution without any marked micro-cracks and pores, following the similar trend as in the previous report.[17]

Table 2. Variation of average grain size, transition temperature, resistivity at room and transition temperature and dielectric constant measurements for the solid solution of $(Ba_{1-x}Bi_X)$ $(Y_xTi_{1-x})O_3$ samples.

Value of x in $(Ba_{1-x}Bi_X)$ $(Y_xTi_{1-x})O_3$	Average grain size (μm)	Transition temperature T_c (°C)	Resistivity at room temperature ρ ($\times 10^7\Omega$-cm)	Resistivity at T_c, 50 Hz ρ ($\times 10^7\Omega$-cm)	Dielectric constant at room temperature (35°C)	Dielectric constant at transition temperature, T_c
$X = 0.00$	1.74	120	3.75	3.94	431	887
$X = 0.01$	1.36	150	1.14	1.41	704	1685
$X = 0.03$	0.59	145	2.19	2.64	621	1128
$X = 0.05$	1.85	125	1.99	2.95	480	971

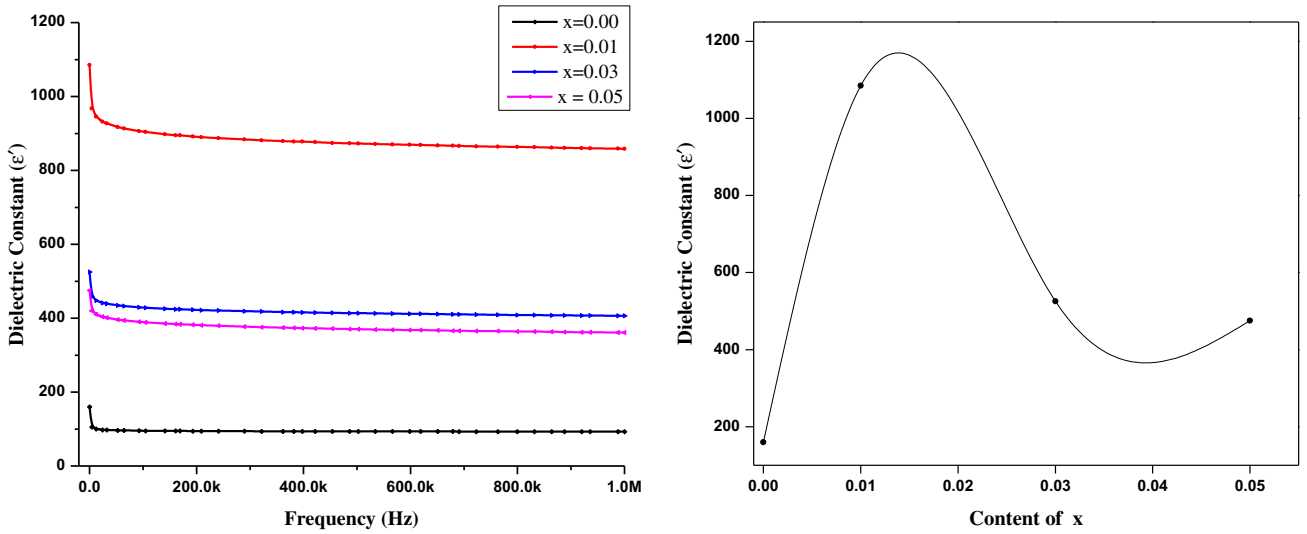

(a) (b)

Fig. 3. (a) The frequency dependent dielectric response for $(Ba_{1-x}Bi_X)$ $(Y_xTi_{1-x})O_3$ ceramics, (b) Variation of dielectric constant (ε') as a function of doping content, x (where $x = 0.00, 0.01, 0.03, 0.05$) at 50 Hz.

3.3. *Dielectric properties*

3.3.1. *Frequency dependence of dielectric properties*

Frequency dependence of dielectric constant were analyzed and given in Fig. 3(a) to show the effect of co-doping on the behavior of BT. The dielectric constant (ε') of Bismuth and Yttrium co-doped barium titanate at room temperature have been measured by using the formula[18]

$$\varepsilon' = \frac{cd}{\varepsilon_o A}, \tag{1}$$

where c refers to capacitance, d the thickness, A the cross-sectional surface area of the pellets in m^2 and ε_o is the permittivity of the free space.[19] We observed, at low frequency, the dielectric constant for all the samples avails higher value[20] and decreases as the frequency increases, then becomes constant at certain frequency having usual dielectric peaks. Therefore, at low frequencies, the effect of microstructure has a direct influence on the dielectric properties of doped BT as previously described.[14]

Figure 3(b) shows variation of dielectric constant (ε') of $(Ba_{1-x}Bi_X)$ $(Y_xTi_{1-x})O_3$ samples with $x = 0.00$, 0.01, 0.03, 0.05 in the frequency range 40 Hz to 1 MHz measured at room temperature. A significant difference was observed in dielectric behavior between low and heavily doped samples. Furthermore, an increase in ε' was observed at all frequencies for all doping concentration of co-doped BT than un-doped BT as expected. The value of ε' decreases as the frequency increases following a general behavior of a dielectric ferroelectric.[5] A higher value of the relative dielectric constant at low frequency is due to the presence of all types of polarizations (i.e., electronic, ionic, dipolar, interfacial, etc.) in the samples at room temperature. Since only electronic polarization dominates at the higher frequency i.e., other types of polarizations vanish. As a result, the ε' value is suppressed.[17] This dielectric behavior can be interpreted by Maxwell–Wagner phonological theory for interfacial polarization and compliance with Koop's theory. The maximum ε' value were observed for $x = 0.01$ concentration and the trend of curve is similar to work of Shaikh *et al.*[19] This also corresponds with the effect of grain size described at Table 1 where the grain size was also finer in case of $x = 0.01$. Compared to un-doped BT lower ε' can be attributed for the presence of porosity which inhibited the motion of the domain wall inside grain.[19]

Dielectric loss ($\tan\delta$) for all samples was measured in the frequency range 40 Hz to 1 MHz at room temperature are given in Fig. 4. $\tan\delta$ is a parameter of a dielectric material that quantifies its inherent dissipation of electromagnetic energy. The loss of energy as heat causes due to electrical conduction and orientational polarization of matter. The

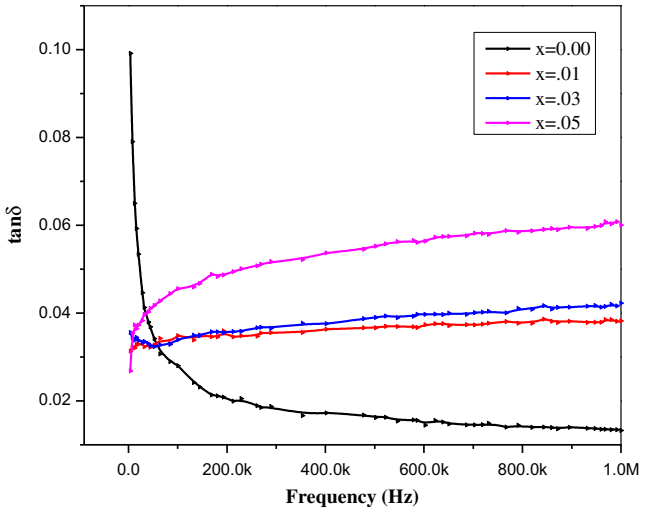

Fig. 4. Dielectric loss (tanδ) as a function of frequency for $(Ba_{1-x}Bi_X)$ $(Y_xTi_{1-x})O_3$ ceramics.

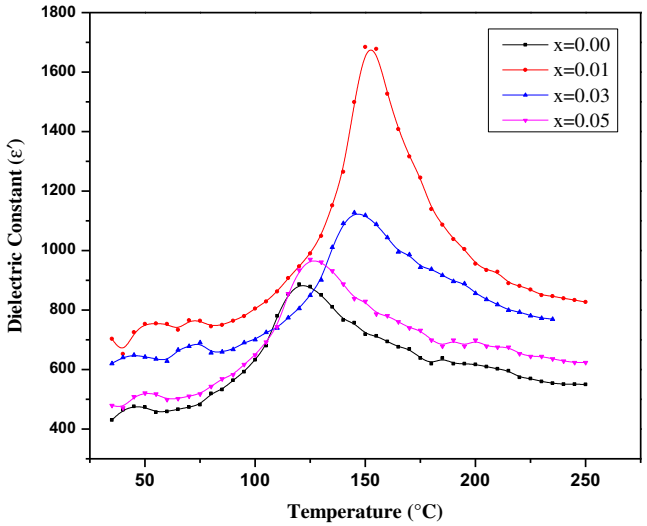

Fig. 5. Temperature dependence of dielectric constant for $(Ba_{1-x}Bi_X)$ $(Y_xTi_{1-x})O_3$ ceramics measured at 50 Hz.

change in tanδ exhibits the same tendency as that of dielectric constant with frequency. At lower frequency tanδ is higher for un-doped BT and it remains lower for co-doped samples. The direction of electron cannot follow the applied field at higher frequency results low dielectric loss.[21] In our study loss tangent shows a good agreement with the dielectric constant where tanδ decreases with the increase in doping concentration.

3.3.2. *Temperature dependence of dielectric properties*

Temperature dependence of dielectric constant (ε') for un-doped and co-doped $BaTiO_3$ samples in the temperature range 35–250°C at 50 Hz frequency are shown in Fig. 5. The results followed a general trend of the ferroelectric property i.e., the dielectric constant increases with the rise in temperature.[22] At Curie temperature, T_c it reaches to its maximum value then undergoes a phase transition from ferroelectric to paraelectric phase. All the samples exhibited a little change in dielectric characteristics. In response to ε', a sharp phase transition from ferroelectric to paraelectric at T_c are observed for low doped ($x = 0.01$) samples. Comparatively broad and stable response were observed for higher dopant concentration for $x = 0.03$ and 0.05.

The dielectric parameters calculated for pure and co-doped BT is given in Table 2. It is observed the Curie peak of BT shifted by co-doping with Bi and Y. Furthermore, the T_c rises upto 150°C at $x = 0.01$ showing a sharp peak. Samples with $x = 0.03$ and 0.05 also exhibit higher T_c and sharper peaks than un-doped BT. In addition, samples with $x = 0.03$ and 0.05 show lower dielectric permittivity compared to the samples with $x = 0.01$. This might be due to the formation of secondary unusual grains. It is evident that secondary grains lead to a decrease in dielectric constant.[22] Another reason could be the segregation of heavily doped Bi and Y in the shell boundary, which makes the shell grain thicker. These kinds of thicker shell grains are responsible for the formation of nanoferroelectric phases. However, in Bi and Mn co-doped BT ceramics, when the ratio of Bi/Mn increased, peak value of ε' decreases with a flattened curve observed.[23] It can be attributed that microstructure and porosity are responsible for the curie peak shifting at higher ε'.[24] Moreover, it is evident that the measured ε' executed proportional approach to relative X-ray density as depicted in Table 1. Variation of Dielectric constant and variation of Curie temperature with doping content x follow the same trend. Again, the dielectric constant ε' increases with increasing x throughout the measuring temperature range. At T_c, it showed higher values, we found 887 for un-doped BT and maximum 1685 for Bi and Y co-doped samples for $x = 0.01$, which is promising. The observed variation in ε' could be associated with the porosity and nonuniform compositional structure and nonhomogeneous distribution of dopant throughout the samples.

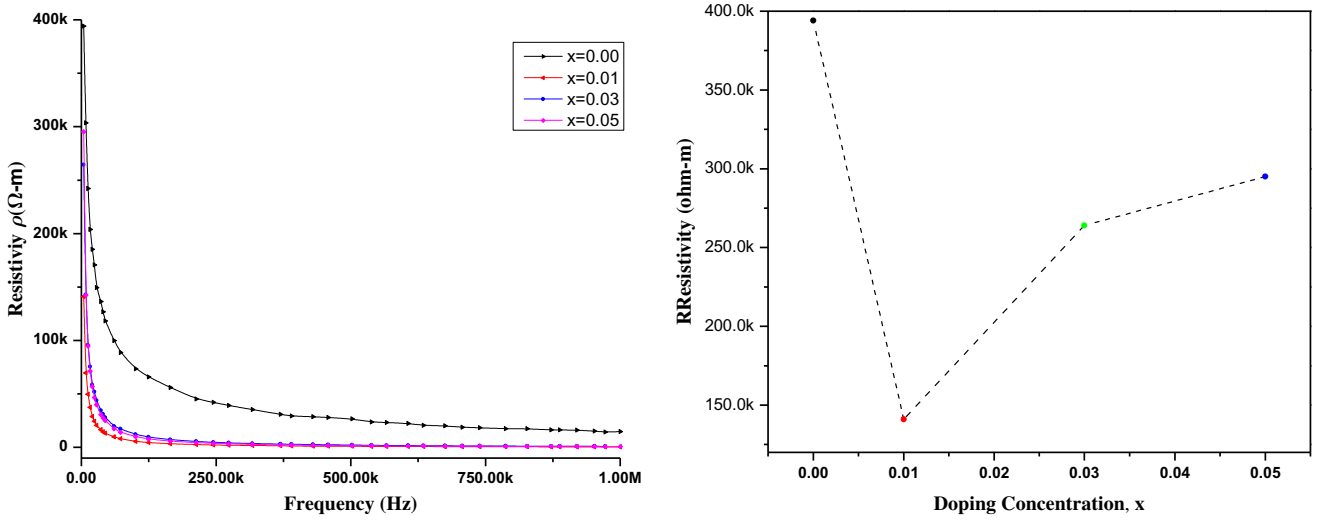

Fig. 6. (a) Frequency-dependent resistivity (ρ) of the $(Ba_{1-x}Bi_X)$ $(Y_xTi_{1-x})O_3$ samples, and (b) Variation of resistivity (ρ) due to doping concentration, x (where $x = 0.00, 0.01, 0.03, 0.05$).

3.4. *Electrical property*

3.4.1. *Frequency dependence of AC resistivity*

Frequency-dependent variation of the electrical resistivity (ρ) of all the prepared samples are measured in the frequency range of 40 Hz to 1 Mz as shown in Fig. 6(a).

We observed that resistivity experiences a steep decreasing trend up to 110 KHz frequency range and becomes independent of frequency afterwards. It can be attributed that in the low frequency range, hopping effect of random charge carriers lowers the resistivity. Independent frequency ranges may be associated with direct current (DC) conductivity ($1/\rho$) at low frequencies, whereas at high frequency range it was attributed as AC conductivity of the system.[25] Similarly, the resistivity showed a higher magnitude with an increased doping concentration of Bi and Y at low frequency range, decreasing trend for co-doped samples (maximum at $x = 0.01$) than un-doped ones. Figure 6(b) illustrates the variation of resistivity (ρ) due to doping concentration, x (where $x = 0.00, 0.01, 0.03, 0.05$). Furthermore, with the increase in doping content x, the resistivity of the samples follows similar trend reported by Paunovic *et al.*[22] It can be attributed that the resistivity becomes almost constant at higher frequencies due to Space charge polarization.

3.4.2. *Temperature dependence of DC electrical resistivity*

The electrical behavior of Bi and Y doped $BaTiO_3$ were analyzed by resistivity versus temperature curves. The DC resistivity was measured as a function of temperature for all the samples. The following relation was used to calculated the resistivity (ρ):

$$R = \rho \frac{L}{A}, \tag{2}$$

where A is the cross-sectional area of the sample and L is the length separating the contacts. The $\ln(\rho)$ versus $1000/T$ graph in Fig. 7 showed that the resistivity increases with the temperature up to 120°C for un-doped BT samples and then decreases.

The experimental data showed that T_c increases with increasing Bi-Y co-doping, however maximum was found at $x = 0.01$ concentration. The resistivity for un-doped BT is $3.94 \times 10^7\Omega$-cm with corresponding grain size of 1.74 μm. The resistivity of BT depends on the grain size, resistivity decreases when grain size increases.[22] It is observed that, the value of resistivity decreases significantly upto $x = 0.01$ followed by further marginal decrease with the increasing of doping content.[26] However, at sample $x = 0.03$, the resistivity found $2.19 \times 10^7\Omega$-cm with a corresponding grain size of 0.59 μm. The variation of average grain size, resistivity, dielectric constant

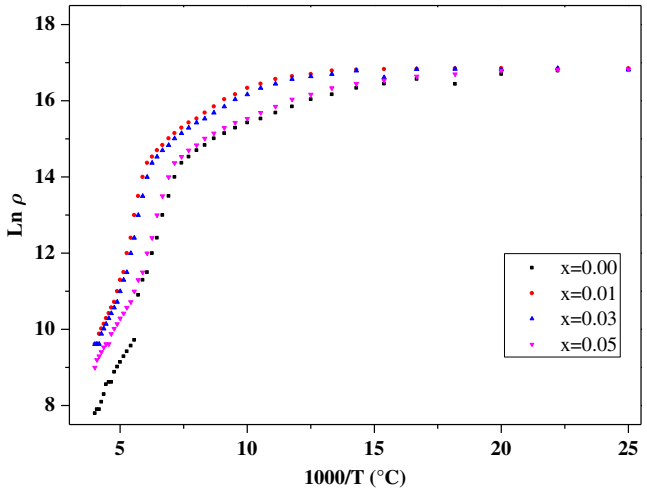

Fig. 7. Temperature dependence resistivity of $(Ba_{1-x}Bi_X)(Y_xTi_{1-x})O_3$ samples.

at room and transition temperature for all prepared samples were represented in Table 2.

4. Conclusions

In this research, both un-doped and co-doped $BaTiO_3$ ceramics have been synthesized at 1300°C sintering temperature for 3 h. It was revealed that the structural, dielectric and electrical properties of $BaTiO_3$ have significant influence on Bismuth and Yttrium co-doping. The XRD pattern confirms perovskite-type structure with tetragonal symmetry. However, with increasing doping concentration, a pseudo cubic phase occurs. The average grain size estimated from SEM micrographs varies significantly due to doping content, which also complies with the XRD results. Considerably higher dielectric constant ε' was found with maximum ∼1685, for $x = 0.01$ in the lower applied frequency range. Furthermore, temperature-dependent ε' result revealed that T_c raised to 150°C for $x = 0.01$ with a sharp peak, but at higher doping content it decreased and became diffused. Frequency-dependent electrical resistivity exhibits a steep decreasing trend up to 110 KHz frequency range and becomes independent of frequency afterwards. The DC resistivity decreases notably with increasing temperature for all compositions of co-doped BT.

Acknowledgments

The authors acknowledge Bangladesh Council of Scientific and Industrial Research (BCSIR) authority for providing the grant for doing this R and D work. They are also thankful to the Director, BCSIR Laboratories, Dhaka and all Scientists and members of Industrial Physics Division, BCSIR, for their co-operation in this research work.

References

1. A. Bussmann-Holder, *J. Phys.: Condens. Matter* **24**, 27 (2012).
2. C. A. Randall, R. E. Newnham and L. E. Cross, *History of the First Ferroelectric Oxide, BaTiO3* (Materials Research Institute, The Pennsylvania State University, University Park, 2004).
3. S. Pradhan and G. S. Roy, *Researcher* **5**, 3 (2013).
4. S. N. Rahman, N. A. Ahmed, N. Khatun and S. Islam, *Int. J. Emerging Technol. Comput. Appl. Sci. (IJETCAS)* **7**, 1 (2014).
5. S. Islam, A. Siddika, N. A. Ahmed, N. Khatun and S. N. Rahman, *Am. Int. J. Res. Sci., Technol., Eng. Math. (AIJRSTEM)* **1**, 28 (2016).
6. S. Islam, A. Siddika, N. Khatun, M. S. Hossain, M. H. A. Begum and N. Ahmed, *Int. J. Nanoelectronics Mater.* **11**, 419 (2018).
7. A. A. Ali, W. M. Faisal and S. K. J. Al-Ani, *Int. J. Nanoelectronics Mater.* **10**, 1 (2017).
8. V. Paunovic, L. Živkovic, L. Vracar, V. Mitic and M. Miljkovic, *Ser. J. Electr. Eng.* **1**, 89 (2004).
9. M. M. Vijatović, J. D. Bobić and B. D. Stojanović, *Sci. Sinter.* **40**, 235 (2008).
10. N. Kumada, H. Ogiso, K. Shiroki, S. Wada, Y. Yonesaki, T. Takei and N. Kinomura, *Mater. Lett.* **64**, 383 (2010).
11. C. E. Lee, S. H. Kang, D. S. Sinn and H. I. Yoo, *J. Electroceram.* **13**, 785 (2004).
12. W. C. Yang, C.-T. Hu and I.-N. Lin, *J. Eur. Ceram. Soc.* **24**, 1479 (2004).
13. T. Badapanda, V. Senthil, D. K. Rana, S. Panigrahi and S. Anwar, *J. Electroceram.* **29**, 117 (2012).
14. R. E. Nettleton, *Ferroelectrics* **1**, 127 (1971).
15. B. Chui, P. Yu, J. Tian, H. Guo and Z. Chang, *Mater. Sci. Eng. A.* **667**, 454 (2006).
16. M. S. Hossain, Y. Akter, S. Mohammad, M. S. Bashar, M. H. A. Begum, M. M. Hossain, S. Islam, N. Khatun and M. A. Mamun, *J. Adv. Dielectr.* **9**, 2 (2019).
17. A. Mansuri, I. N. Bhatti and A. Mishra, *J. Adv. Dielectr.* **8**, 4 (2018).
18. C. Kittle, *Introduction to Solid State Physics* (Wiley, Newyork, 1995).
19. A. Shaikh and Y. D. Kolekar, *J. Anal. Appl. Pyrol.* **93**, 41 (2012).
20. D. Y. Lu, X. Y. Sun and M. Toda, *J. Phys. Chem. Solids* **68**, 650 (2007).

21. J. Zhi, A. Chen, Y. Zhi, P. M. Vilarinho and J. L. Baptista, *J. Am. Ceram. Soc.* **82**, 5 (1999).
22. V. Paunovic, L. J. Zivkovic and V. Mitic, *Sci. Sinter.* **42**, 69 (2010).
23. D. Shihua, S. Tianxiu, Y. Xiaojing, L. Xiaobing and L. Guobiao, *Ceram. Int.* **38** (2012).
24. K. Shiroki, N. Kumada, H. Ogiso, Y. Yonesaki, T. Takei, N. Kinomura and S. Wada, *Mat. Sci. Eng.* **18**, 9 (2011).
25. M. Borah and D. Mohanta, *Appl. Phys. A* **115**, 1057 (2014).
26. R. Islam, S. Chowdhury, S. N. Rahman and M. J. Rahman, *J. Ceram. Process. Res.* **13**, 248 (2012).